

# Clustering of Extragalactic Sources from 151 MHz to 232 MHz: Implications for Cosmological 21-cm Observations

Angélica de Oliveira-Costa<sup>1</sup> & Joseph Lazio<sup>2,3</sup>

<sup>1</sup>Harvard-Smithsonian Center for Astrophysics, Cambridge, MA 02138, USA

<sup>2</sup>Naval Research Laboratory, Washington, DC 20375, USA

<sup>3</sup>NASA Lunar Science Institute, NASA Ames Research Center, Moffett Field, CA

30 October 2018. To be submitted to MNRAS.

## ABSTRACT

In order to construct accurate point sources simulations at the frequencies relevant to 21-cm experiments, the angular correlation of radio sources must be taken into account. This paper presents a measurement of angular two-point correlation function,  $w(\theta)$ , at 232 MHz from the MIYUN survey – tentative measurements of  $w(\theta)$  are also performed at 151 MHz. It is found that double power law with shape  $w(\theta) = A\theta^{-\gamma}$  fits the 232 MHz data well. For the angular length of  $0.2^\circ \lesssim \theta \lesssim 0.6^\circ$ ,  $\gamma \approx -1.12$ , and this value of slope is independent of the flux-density threshold; while for angular lengths much greater than 0.6,  $\gamma$  has a shallower value of about  $-0.16$ . By comparing the results of this paper with previous measurements of  $w(\theta)$ , it is discussed how  $w(\theta)$  changes with the change of frequency and completeness limit.

**Key words:** cosmology – methods: data analysis – astronomical data bases: miscellaneous

## 1 INTRODUCTION

There has been considerable recent interest in using the highly redshifted hyperfine line from HI (21-cm line) for astrophysical and cosmological studies at redshifts  $z > 6$  (Pritchard & Loeb 2008). At these redshifts, the 21-cm line is redshifted to metre wavelengths, and extracting the cosmological signature requires accurate modeling and removal of the foreground Galactic and extragalactic emission (Santos et al. 2005; Morales et al. 2005; Wang et al. 2006).

The diffuse Galactic foreground emission fluctuates mainly on large angular scales (de Oliveira-Costa et al. 2008), or on scales that are much larger than the expected angular fluctuations of the 21-cm signal. Point source contamination from discrete extragalactic radio source, on the other hand, affects mainly small angular scales and potentially could be more problematic. A number of surveys of radio sources have been performed at frequencies relevant to the 21-cm tomography – see Figure 1 in (Cohen et al. 2003); and analysis of these catalogs have helped to bring some understanding about their statistical properties: for instance, it is known that the distribution of radio sources obeys a Poisson statistics with an observed angular clustering – see Table 1<sup>1</sup>.

In this respect, our knowledge of the extragalactic radio source clustering properties is important because, if there is clustering on small angular scales, it could contribute power to a power

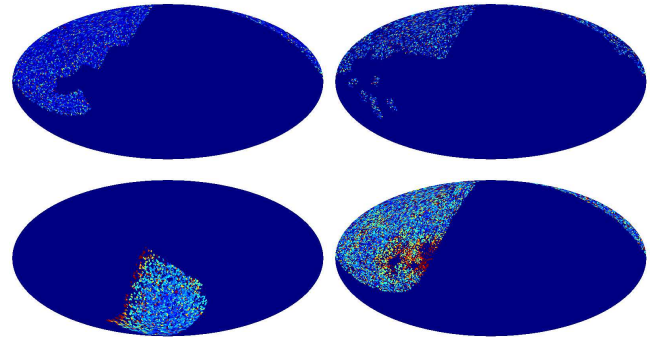


**Figure 1.** Footprints of the 6C 151 MHz catalogue (*top, left*), the 7C 151 MHz catalogue (*top, right*), the MRT 151 MHz catalogue (*bottom, left*) and the MIYUN 232 MHz catalogue (*bottom, right*). All footprints were computed using the HEALPix projection (Gorski et al. 2005), on which locations covered by the catalogues are in a brighter color (we adopted the convention in which an increase in flux density  $S$  corresponds to an increase in color's brightness). All catalogues are plotted in the interval of  $0 \leq S \leq 1$  Jy, and in Galactic coordinates with the Galactic center at the origin and longitude increasing to the left.

spectral analysis; as a result, the clustering signal could be confused with the 21-cm signal that is being sought. Further, in order to construct accurate simulations at metre wavelengths<sup>2</sup>, the

<sup>1</sup> The range of frequencies we consider in this analysis correspond to a redshift range  $z \approx 6-8$ , which are well within the range being considered for the Epoch of Reionization.

<sup>2</sup> Some aspects of both experimental design optimization and ac-

angular correlation of radio sources must be taken into account (Gonzalez-Nuevo et al. 2005). At the faint flux densities relevant for 21-cm cosmological studies, the relative importance of the clustering contribution increases and could become an important contribution to power spectral analyses.

This paper presents a measurement of angular two-point correlation function  $w(\theta)$  at 232 MHz and a tentative measurement at 151 MHz. By comparing the results of this paper with previous measurements of  $w(\theta)$ , we assess how  $w(\theta)$  changes with the change of frequency and completeness limit. In Section 2, we describe the statistical tools as well as the surveys used in this analysis. The results and conclusions are presented in Sections 3 and 4, respectively.

## 2 DATA ANALYSIS TOOLS

### 2.1 The Angular 2-point Correlation Function

The clustering of astronomical sources is quantified using the angular two-point correlation function  $w(\theta)$ . One way to estimate this function is to compare the distribution of the objects in the real catalogue to the distribution of points in a random Poisson distributed catalogue with the same boundaries (Hamilton 1993), or

$$w(\theta) = \frac{DD(\theta) * RR(\theta)}{[DR(\theta)]^2} - 1 \quad (1)$$

where  $DD(\theta)$ ,  $RR(\theta)$  and  $DR(\theta)$  are the numbers of data-data, random-random and data-random pairs separated by the distance  $\theta + \delta\theta$ .

The estimation of  $RR(\theta)$  and  $DR(\theta)$  requires a catalogue of objects distributed uniformly over an area with the same angular boundaries as the data catalogue. In order to produce such catalogues, we used the ‘‘Sphere Point Picking Algorithm’’<sup>3</sup> to generate random cartesian vectors equally distributed on the surface of a unit sphere (to avoid having vectors ‘‘bunched’’ around the poles, as would happen if spherical coordinates were used). See (de Oliveira-Costa & Capodilupo 2009) for more details on how these catalogues were produced.

Incomplete knowledge of the completeness limit of a survey can affect our determination of the extent of clustering (Magliocchetti et al. 1998). If a completeness limit for a given survey cannot be found in the literature, we estimate a *ballpark* value from the survey’s differential source counts  $dN/dS$ . We derive  $dN/dS$  by binning the sources in flux density with bins of 0.1 in width, and the bins are not weighted by  $S^{-2.5}$ .

### 2.2 The Catalogues

All the catalogues described in this subsection are available at <http://vizier.cfa.harvard.edu/viz-bin/VizieR>, and are shown in Figure 1. Below we provide a brief description of the data sets used in this analysis.

tual data analysis require full-blown simulations of the sky signal and knowledge about how it propagates through the instrument and the data analysis pipeline. End-to-end simulations are important for 21-cm experiments because of the many complicated issues related to instrumental performance, ionospheric turbulence corrections, etc. (Morales & Hewitt 2004; Bowman et al. 2006; Morales et al. 2005; Bowman 2007; Bowman et al. 2009).

<sup>3</sup> <http://mathworld.wolfram.com/SpherePointPicking.html>.

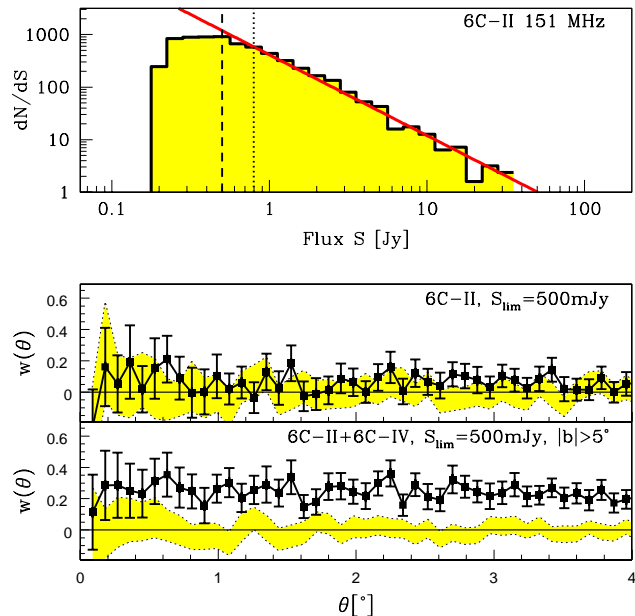


**Figure 2.** The measured source counts  $dN/dS$  (top) and angular correlation function  $w(\theta)$  (middle, bottom) of the 6C 151 MHz catalogue. *Top:* The source count of the 6C-II region is plotted using the peak amplitudes. The red line is a single power law fit to the histogram (black line), for which  $dN/dS = 2.61 - 1.54S$ . *Middle:* The angular correlation function of the 6C-II region calculated for a flux density limit of  $S = 500$  mJy. *Bottom:* The angular correlation function of the (6C-II + 6C-IV) region calculated for a flux density limit of  $S = 500$  mJy, restricting to Galactic latitudes  $|b| > 5^\circ$ . The yellow shaded regions in the *middle* and *bottom* panels represent  $w(\theta)$  calculated using solely mock catalogues.

The 6<sup>th</sup> Cambridge (6C) survey produced a catalogue of radio sources at 151 MHz with 34,418 discrete sources at an angular resolution of  $4.2' \times 4.2' \text{ csc}(\delta)$ . The data product is a set of seven sections (named 6C-I, 6C-II, 6C-III, 6C-IV, 6C-Va, 6C-Vb, and 6C-VI) that maps the sky north of  $+30^\circ$  declination, with limiting flux densities between 130 mJy and 200 mJy, depending on the section analysed (Baldwin et al. 1985; Hales et al. 1988; Hales et al. 1990; Hales et al. 1991; Hales et al. 1993a; Hales et al. 1993b). The uncertainties on the positions and flux densities of many sources in the regions 6C-Va, 6C-Vb and 6C-VI are not well quantified (Hales et al. 1993a; Hales et al. 1993b), so we exclude these regions from our analysis.

The 7<sup>th</sup> Cambridge (7C) survey produced a catalogue of radio sources at 151 MHz with 43,683 discrete sources at an angular resolution of  $1.2' \times 1.2' \text{ csc}(\delta)$ . This survey is composed by combining 96 individual images at declinations greater than  $+21^\circ$ . These images have completeness limits between 120 mJy and 770 mJy, depending on the image analysed (Hales et al. 2007).

The Mauritius Radio Telescope (MRT) is a Fourier synthesis array that has produced images of the sky covering the region  $18^h < \alpha < 24^h$  and  $-75^\circ < \delta < -10^\circ$  (Nayak et al. 2009). The resulting catalogue contains 2,784 discrete sources at an angular resolution of  $4.6' \times 4.6'$  with a completeness limit<sup>4</sup> of about 1 Jy.

The MIYUN 232 MHz survey mapped the sky north of declination  $+30^\circ$  at an angular resolution of  $3.8' \times 3.8' \text{ csc}(\delta)$ , with an average noise level of 50 mJy. The principal data product

<sup>4</sup> Shankar 2009, private communication.

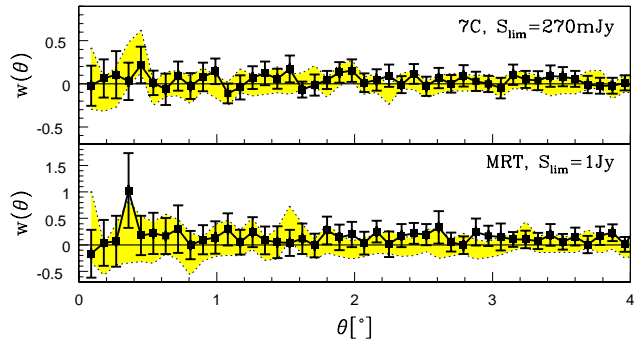


**Figure 3.** Measured angular correlation function  $w(\theta)$  of the 7C (*top*) and MRT (*bottom*) 151 MHz catalogues. The angular correlations are calculated at the flux density limit of  $S = 270$  mJy (7C) and  $S = 1$  Jy (MRT). The yellow shaded region is  $w(\theta)$  calculated using solely mocks.

of this survey is a catalogue containing 34,426 discrete sources (Zhang et al. 1997), complete at the 250 mJy level (Zhang 1999).

### 3 RESULTS

#### 3.1 The catalogues at 151 MHz: 6C, 7C, & MRT

The completeness limits of the 6C-I, 6C-II, 6C-III, and 6C-IV regions were not published. Using the source counts  $dN/dS$ , as described in §2.1, we estimate completeness limits of 200 mJy, 500 mJy, 250 mJy, and 500 mJy, respectively. Figure 2 illustrates our estimation procedure. The top panel shows the differential source count (peak amplitudes) of the 8,275 objects in the 6C-II region. The red line corresponds to a single power law fit to the  $dN/dS$  distribution, for which  $dN/dS = 2.61 - 1.54S$ . At flux densities below 800 mJy (vertical black dotted line), the number counts begin to flatten, and the lack of faint objects becomes very important below 500 mJy (vertical black dashed line). We conclude that this survey region is incomplete at flux densities below 500 mJy.

Figure 2 (middle) shows the measured  $w(\theta)$  of the 6C-II region for our assumed completeness limit of 500 mJy. The measured correlations are represented by the black squares<sup>5</sup>, and distances between data and/or random sources are measured in bins of  $0.09^\circ$ . At this flux density limit, the 6C-II catalogue contains 4,111 objects. The results are consistent with zero. Similar results were obtained for the three remaining regions 6C-I, 6C-III, and 6C-IV. We also investigated if  $w(\theta)$  changes with a change in bin size, in Galactic latitude cut, or flux density limit. There is no indication that modest changes in any of these quantities affect the results.

<sup>5</sup> In order to avoid having Galactic sources in our analysis, we adopted Galactic latitude limits and discarded sources at lower Galactic latitudes before measuring  $w(\theta)$ . 100 mock catalogues are constructed using the procedure described in §2.1, with flux densities above the sensitivity limit of the data catalogue and a chosen Galactic latitude cut (if applicable). By cross-correlating the data with the 100 mocks, a set of normally distributed estimates of the correlation function is produced. The mean and the standard deviation of this distribution are used as a value for the estimate and its uncertainty in the measurement of  $w(\theta)$  at each  $\theta$ . The estimate (mean) and its uncertainty (the standard deviation) are shown as the black squares and their uncertainties (*e.g.*, Figure 2, middle). Similarly, the 100 mocks are correlated with themselves. This result corresponds to the yellow shaded region shown in the correlation figures, and, as expected in a Poissonian distribution,  $w(\theta)$  is consistent with zero.

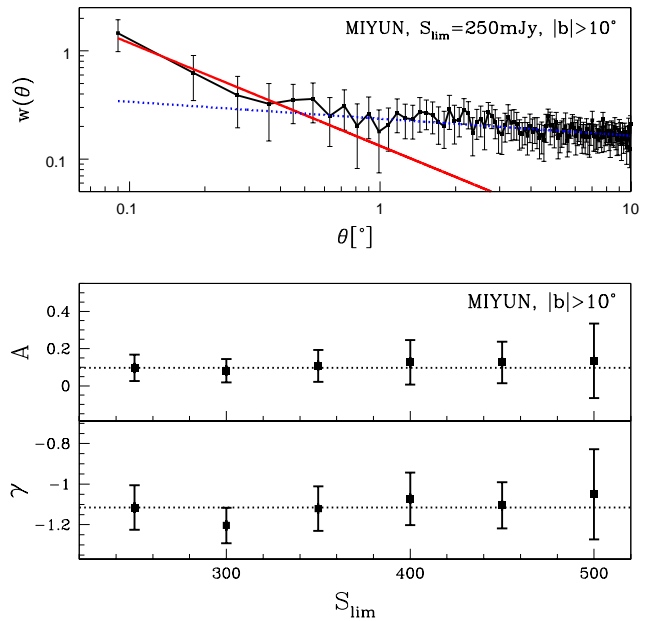


**Figure 4.** The angular correlation function  $w(\theta)$  and the amplitudes  $A$  and power law indices  $\gamma$  as a function of flux density determined from the 232 MHz MIYUN catalogue. *Top*: The angular correlation function is calculated for a flux density limit of 250 mJy, for a Galactic latitude cut of  $10^\circ$ . The red solid and the dashed blue lines are single power laws that fit the data, with  $w(\theta) = A\theta^{-\gamma}$ . *Middle and Bottom*: The amplitudes  $A$  and power law indices  $\gamma$  are measured for various flux density limits from 250 mJy to 500 mJy, in steps of 50 mJy. The amplitude of clustering does not depend on flux density.

As an extra test,  $w(\theta)$  was measured over grouped survey regions with similar completeness limits. Figure 2 (bottom) shows  $w(\theta)$  calculated for the combined (6C-II + 6C-IV) region, with a completeness limit of 500 mJy and a Galactic latitude cut of  $5^\circ$ . At this flux density limit, the (6C-II + 6C-IV) catalogue contains 6,806 objects, extending from  $+30^\circ$  to  $+82^\circ$  in declination. The data show the presence of a large scale correlation (which extends beyond  $10^\circ$ ), but no signs of small scale ( $\theta < 1^\circ$ ) clustering. As discussed by (Blake & Wall 2002), a possible explanation for this large-scale correlation is a varying areal density of sources on the sky, such as might occur from combining two 6C survey regions. In the case of 6C-II and 6C-IV, the former covers a declination range of  $+50^\circ$  to  $+51^\circ$  while the latter covers  $+67^\circ$  to  $+82^\circ$ . The change in *projected* interferometric baselines over this range of declinations would produce a varying surface brightness sensitivity, which in turn could affect the density of sources on the sky, and thereby spuriously enhance the measured value of  $w(\theta)$ .

Like the 6C catalogue, the 7C catalogue was extracted from a survey composed by multiple individual images that have completeness limits varying between 120 mJy and 770 mJy (Hales et al. 2007). Therefore,  $w(\theta)$  was measured in each individual region, as well as in aggrouped regions having the same completeness limit. Figure 3 (top) shows an example of the resulting angular correlation function for a region with a completeness limit of 270 mJy. At this flux density limit, the catalogue contains 2,872 objects. Distances between data and/or random sources are measured in bins of  $0.09^\circ$ . The results are consistent with zero. Similar results were obtained for the other regions in the 7C catalogue. We also investigated whether  $w(\theta)$  changed with a (modest) change in

**Table 1.** Published  $w(\theta)$ <sup>1</sup> values.

Ref	$\nu$ [GHz]	$A$	$\gamma$	$w(\theta)$ [ $\square$ ]	$S_{\text{lim}}$ [mJy]
(de Oliveira-Costa & Capodilupo 2009)	0.074	$0.103 \pm 0.026$	$1.21 \pm 0.35$	0.2–0.6	770
This Work (6C)	0.151			–	500
This Work (7C)	0.151			–	120–770
This Work (MRT)	0.151			–	1000
This Work (MIYUN, $ b  > 10^\circ$ )	0.232	$0.096 \pm 0.071$	$1.12 \pm 0.11$	$< 0.6$	250
$A \times 10^{-3}$					
(Seldner & Peebles 1981)	0.178			1.50–3.0	3000
(Rengelink & Rottgering 1999)	0.325	$2.0 \pm 0.5$	0.8	$< 1.0$	35
(Blake et al. 2004)	0.325	$1.01 \pm 0.35$	$1.22 \pm 0.33$	$> 0.2$	35
(Webster 1977a)	0.408			–	250
(Webster 1977b)	0.408			–	10
(Blake et al. 2004)	0.843	$2.04 \pm 0.38$	$1.24 \pm 0.16$	$> 0.2$	10
(Cress et al. 1996)	1.400	$3.7 \pm 0.3$	$1.06 \pm 0.03$	0.02–2.0	3
(Magliocchetti et al. 1999)	1.400	$2.68 \pm 0.07$	$1.52 \pm 0.06$	0.30–3.0	3
(Overzier et al. 2003)	1.400	$1.2 \pm 0.1$	1.8	$> 0.3$	3
(Blake et al. 2004)	1.400	$1.49 \pm 0.15$	$1.05 \pm 0.10$	$> 0.3$	10
(Overzier et al. 2003)	1.400	$1.0 \pm 0.2$	1.8	$> 0.3$	10
(Webster 1977a)	2.700			–	350
(Sicotte & Peebles 1995)	4.850			0.70–1.7	45
(Kooiman et al. 1995)	4.850	4.01	0.8	0.30–1.9	35
(Rengelink & Rottgering 1999)	4.850	$6.5 \pm 2.0$	0.8	$< 2.5$	35
(Loan et al. 1997)	4.850	$10.0 \pm 5.0$	0.8	$< 2.0$	50

<sup>1</sup> $w(\theta)$  is fitted by a power-law of the form  $A\theta^{-\gamma}$   
 $S_{\text{lim}}$  is the limiting flux density.

bin size or Galactic latitude cut, and there is no indication that any of these changes affect the results.

Figure 3 (bottom) shows the measurement of  $w(\theta)$  for the MRT catalogue, with a flux density limit of 1 Jy (black squares). At this flux limit, the catalogue contains 2,294 objects. Distances between data and/or random sources are measured in bins of  $0.09^\circ$ . The results are consistent with zero. We also investigated whether  $w(\theta)$  changed with a (modest) change in bin size, flux density limit, or Galactic latitude cut, and there is no indication that any of these changes affect the results.

### 3.2 The MIYUN catalogue

Figure 4 (top) shows the determination of  $w(\theta)$  for the flux density limit of 250 mJy (black squares). Distances between data and/or random sources are measured in bins of  $0.09^\circ$ . It is apparent that the angular correlation function cannot be fit with a single power law, but requires two power laws, each of the form  $w(\theta) = A\theta^{-\gamma}$  (Peebles 1980), where  $A$  is a measure of the amplitude of the average enhancement of the number of radio sources at a particular point in the sky. Fitting the data with a double power law model yields a weak correlation with  $A = 0.096 \pm 0.071$  and  $\gamma = -1.12 \pm 0.11$  (red solid line, with  $\chi^2=0.01$ ), and  $A = 0.236 \pm 0.092$  and  $\gamma = -0.16 \pm 0.05$  (blue dotted line, with  $\chi^2=0.24$ ). The break in the angular correlation function occurs between  $0.4^\circ \lesssim \theta \lesssim 0.6^\circ$ . This break could be the indication that

there is a small angular scale signal (maybe caused by clustering) added to a large angular scale signal in the survey<sup>6</sup>.

We also investigated whether  $w(\theta)$  changed with a (modest) change in bin size or Galactic latitude cut. Variations in the bin size did not affect the results, but for Galactic latitude cuts greater than  $+15^\circ$ ,  $w(\theta)$  is consistent with zero.

The angular correlation function  $w(\theta)$  was also calculated for various flux density limits from 300 to 800 mJy, in increments of 50 mJy. Above the flux density limit of 500 mJy, the correlation for small angular scales ( $\theta < 0.6^\circ$ ) approaches zero. As shown in Figure 4 (*middle* and *bottom*), for a  $10^\circ$  Galactic latitude cut, the amplitude of clustering does not depend on flux density. This same result was observed in previous angular correlation analysis, *e.g.*, (Blake et al. 2004; de Oliveira-Costa & Capodilupo 2009).

## 4 CONCLUSIONS

We have used existing 151 MHz and 232 MHz catalogues to estimate the angular correlation function  $w(\theta)$  relevant for both simulation and analysis of 21-cm cosmological observations. At 151 MHz (corresponding to  $z \approx 8.4$ ), our estimate of  $w(\theta)$  is determined from the 6C, 7C, and MRT surveys. In all cases, the results are consistent with zero, implying no observed clustering of radio sources, at flux density limits ranging from about 0.3 Jy to 1 Jy. At 232 MHz (corresponding to  $z \approx 5$ ), we found that

<sup>6</sup> As pointed out by (Blake & Wall 2002), in a wide-area survey undertaken with an interferometer (such as the MIYUN), large scale gradients in completeness limit typically appear as a function of declination.

$w(\theta)$  can be fit by a two broken power laws, each with shape  $w(\theta) = A\theta^{-\gamma}$ , with a break at an angular scale of  $\theta \sim 0.5^\circ$ . At small angular scales, with a Galactic latitude cut of  $10^\circ$  and a flux density limit of 250 mJy, we find  $A = 0.096 \pm 0.071$  and  $\gamma = -1.12 \pm 0.11$  (with  $\chi^2=0.01$ ), while, at large angular scales, we find  $A = 0.236 \pm 0.092$  and  $\gamma = -0.16 \pm 0.05$  (with  $\chi^2=0.24$ ). The value of  $\gamma$  at small angular scales is consistent with that measured from radio catalogues at higher frequencies (Table 1).

From Table 1, it appears that the power law index  $\gamma$  of the angular correlation function is essentially constant over the frequency range from 74 MHz to 232 MHz ( $20 \lesssim z \lesssim 5$ ), and it is also consistent with that determined from higher frequencies, at least as high as 1400 MHz. Strikingly, however, it is not clear that the angular scales for which this power law index applies are consistent across the range of frequencies: at the lower frequencies, clustering seems to be important on angular scales of  $\theta \lesssim 0.6^\circ$ , while at higher frequencies, the clustering is important on angular scales  $\theta \gtrsim 0.3^\circ$ . These are overlapping ranges, but not entirely consistent.

It is important to point out that the classes of sources being probed at the different frequencies are also not entirely the same. Source counts at 1400 MHz indicate that strong radio sources (*e.g.*, FR II radio galaxies) dominate at flux densities above about 10 mJy, while star forming galaxies become important at lower frequencies. The current flux density limits for surveys at frequencies around 200 MHz (and below) are about 500 mJy. Assuming a nominal spectral index of  $\alpha = -0.7$  ( $S_\nu \propto \nu^\alpha$ ), these flux density limits imply flux densities of about 125 mJy at 1400 MHz, which is well above the flux density limits probed by the surveys around 1000 MHz, and consistent with the notion that the current generation of low-frequency surveys are dominated by powerful radio sources. Consequently, one potential explanation is that the possible inconsistencies are due, in part, to the different source populations being probed. However, it is also notable that the clustering amplitude  $A$  is fairly marginal (always less than  $4\sigma$ , and in some cases consistent with zero) at frequencies lower than 1400 MHz; while at the higher frequencies, by contrast, the clustering amplitudes can exceed a significance of  $10\sigma$ .

For the purposes of 21-cm cosmological observations, either simulating sky models or analyzing low radio frequency observations, we conclude that it is acceptable to scale the angular clustering results from higher to lower frequencies. One caveat to this conclusion is if a strongly clustered, steep-spectrum population of objects exists. Using a fiducial 1400 MHz flux density of 10 mJy allows us to estimate how deep future low-frequency surveys might need to be in order to assess this possible inconsistency (or the existence of a possible steep-spectrum population) in the scale of angular clustering. With the nominal spectral index of  $-0.7$ , we estimate that a survey around 150 MHz<sup>7</sup> would need to reach a limiting flux density of about 50 mJy (implying a thermal noise limit of about 7 mJy).

**ACKNOWLEDGMENTS:** We thank N. Kassim for illuminating discussions. Support for this work was provided by the NSF through grants AST-0607597 and AST-0908950. The LUNAR consortium is funded by the NASA Lunar Science Institute (via Cooperative Agreement NNA09DB30A) to investigate concepts for astrophysical observatories on the Moon. Basic research in radio astronomy at NRL is supported by 6.1 Base funding.

## REFERENCES

- Baldwin J.E., Boysen R.C., Hales S.E.G., Jennings J.E., Waggett P.C., Warner P.J., Wilson D.M.A., 1985, MNRAS, 217, 717  
 Blake C., Mauch T., Sadler E.M., 2004, MNRAS, 347, 787  
 Blake C., Wall J., 2002a, MNRAS, 337, 993  
 Bowman J.D., 2007, “Probing the Epoch of Reionization with Redshifted 21-cm HI Emission”, Ph.D. Thesis, Massachusetts Institute of Technology  
 Bowman J.D., Morales M.F., Hewitt J.H., 2006, ApJ, 638, 20  
 Bowman J.D., Morales M.F., Hewitt J.H., 2009, ApJ, 695, 18  
 Cohen A.S., Rottgering H.J.A., Kassim N.E., Cotton W.D., Perley R.A., Wilman R., Best P., Pierre M., Birkinshaw M., Bremer M., Zanichelli A., 2003, ApJ, 591, 640  
 Cress C.M., Helfand D.J., Becker R.H., Gregg M.D., White R.L., 1996, ApJ, 473, 7  
 de Oliveira-Costa A., Capodilupo J., 2009, arXiv:0908.4248  
 de Oliveira-Costa A., Tegmark M., Gaensler B.M., Jonas J., Landecker T.L., Reich P., 2008, MNRAS, 388, 247  
 Gonzalez-Nuevo J., Toffolatti L., Argueso F., 2005, ApJ, 621, 1  
 Gorski, K.M., Hivon, E., Banday, A.J., Wandelt, B.D., Hansen, F.K., Reinecke, M., Bartelmann, M., 2005, ApJ, 622, 759  
 Hales S.E.G., Baldwin J.E., Warner P.J., 1988, MNRAS, 234, 919  
 Hales S.E.G., Baldwin J.E., Warner P.J., 1993b, MNRAS, 263, 25  
 Hales S.E.G., Masson C.R., Warner P.J., Baldwin J.E., 1990, MNRAS, 246, 256  
 Hales S.E.G., Masson C.R., Warner P.J., Baldwin J.E., Green D.A., 1993a, MNRAS, 262, 1057  
 Hales S.E.G., Mayer C.J., Warner P.J., Baldwin J.E., 1991, MNRAS, 251, 46  
 Hales S.E.G., Riley J.M., Waldram E.M., Warner P.J., Baldwin J.E., 2007, MNRAS, 382, 1639  
 Hamilton A.J.S., 1993, ApJ, 417, 19  
 Kooiman B.L., Burns J.O., Klypin A.A., 1995, ApJ, 448, 500  
 Loan A.J., Wall J., Lahav O., 1997, MNRAS, 286, 994  
 Magliocchetti M., Maddox S.J., Lahav O., Wall J., 1998, MNRAS, 300, 257  
 Magliocchetti M., Maddox S.J., Lahav O., Wall J., 1999, MNRAS, 306, 943  
 Morales M.F., Bowman J.D., Hewitt J.H., 2005, A&AS, 207, 3304  
 Morales M.F., Hewitt J.H., 2004, ApJ, 615, 7  
 Nayak A., Daiboo S., Shankar N.U., 2009, ASPC, 407, 426  
 Overzier R.A., Rottgering H.J.A., Rengelink R.B., Wilman R.J., 2003, A&A, 405, 53  
 Peebles P.J., 1980, “The Large Scale Structure of the Universe”, Princeton University Press  
 Pritchard, J.R., & Loeb, A. 2008, PhRvD, 78, 103511  
 Rengelink R., Rottgering H., 1999, Proc. of the “The Most Distant Radio Galaxies”, Ed. Rottgering H.J.A., Best P.N., Lehnert M.D., Amsterdam, 15-17 October 1997, p. 399  
 Santos M.G., Cooray A., Knox L., 2005, ApJ, 625, 575  
 Seldner M., Peebles P.J.E., 1981, MNRAS, 194, 251  
 Sicotte H., Peebles P.J.E., 1995, AIPC, 336, 390  
 Wang X., Tegmark M., Santos M.G., Knox L., 2006, ApJ, 650, 529  
 Webster A., 1977a, MNRAS, 179, 511  
 Webster A., 1977b, MNRAS, 179, 517  
 Zhang X., 1999, IAUS, 183, 276  
 Zhang X., Zheng Y., Chen H., Wang S., Cao S., Peng B., Nan R., 1997, A&AS, 121, 59

<sup>7</sup> Such as the proposed Million Source Shallow Survey (MSSS) with the Low Frequency Array (LOFAR) – more information at <http://www.astron.nl/general/lofar/lofar>.